

Antiferromagnetic phase transition in $\text{Cd}_{1-x}\text{Mn}_x\text{Se}$ epilayers

T. M. Giebultowicz,* P. Klosowski, N. Samarth, and H. Luo

Department of Physics, University of Notre Dame, Notre Dame, Indiana 46556

J. J. Rhyne

National Institute of Standards and Technology, Gaithersburg, Maryland 20899

J. K. Furdyna

Department of Physics, University of Notre Dame, Notre Dame, Indiana 46556

(Received 16 March 1990)

Neutron-diffraction spectra of molecular-beam-epitaxy (MBE)-grown single-crystal zinc-blende films of $\text{Cd}_{1-x}\text{Mn}_x\text{Se}$ reveal the onset of type-III antiferromagnetic ordering (AFM-III) for $x=0.70$ and 0.75 at a sharp Néel temperature. The AFM-III order is *long range*, with correlation lengths of around 400 \AA , and the transition is of second order. This contrasts sharply with earlier studies of bulk $A_{1-x}B_x$ diluted magnetic semiconductors, where only short-range AFM-III correlations are observed, evolving gradually with decreasing temperature, and saturating at correlation length values less than 70 \AA .

The $A_{1-x}B_x$ diluted magnetic semiconductors (DMS) (Ref. 1) are of fundamental importance to contemporary studies in magnetism because they offer practical examples of strongly frustrated, randomly diluted three-dimensional (3D) Heisenberg antiferromagnets with well characterized and predominantly short-range Mn-Mn exchange interactions.^{2,3} Both the frustration due to the FCC lattice and the random dilution presumably play crucial roles in driving the transition to a dynamically frozen spin-glass-like phase observed in DMS alloys at low temperatures.⁴ The exact nature of this low-temperature phase has been a matter of vigorous debate, especially for moderate and higher Mn concentrations ($x \geq 0.4$), with conflicting dynamical scaling arguments favoring either the formation of a spin-glass⁵ or a random-field magnet.⁶ However, as has been recently shown by using a new approach to critical dynamic scaling,⁷ the $\chi''(\omega, T)$ data from $\text{Cd}_{1-x}\text{Mn}_x\text{Te}$ is clearly consistent with a spin-glass state up to at least $x=0.40$.

The only *direct* microscopic picture of the low-temperature magnetic phase for $x > 0.4$ has so far been provided by elastic neutron-scattering measurements on various $A_{1-x}B_x$ alloys.⁸ These studies have indicated the formation of antiferromagnetically ordered clusters that individually correspond to Anderson's ordering of the third kind (AFM-III). The antiferromagnetic correlation range increases gradually with decreasing temperature, eventually saturating below the "spin-glass" temperature (T_g) at which a cusp is observed in susceptibility measurements. However, even for the highest magnetic concentrations studied so far ($\text{Zn}_{0.32}\text{Mn}_{0.68}\text{Te}$ and $\text{Cd}_{0.30}\text{Mn}_{0.70}\text{Te}$), the antiferromagnetic order is *patently short range*, with a maximum observed correlation length of 70 \AA , and there is *no existing evidence* for an antiferromagnetic phase transition.

Theoretical calculations for randomly diluted, frustrated 2D XY spins² predict a transition to an antiferromagnetic phase for high Mn concentrations. Similar behavior

has been predicted for the frustrated fcc $d=3$ systems such as $A_{1-x}B_x$ alloys, although analytic calculations have only dealt with the weakly diluted case.⁹ The only explicit predictions of a critical concentration x_c for a transition from short-range order (SRO) to long-range order (LRO) in DMS systems are based on numerical calculations,¹⁰ and these are suspect due to the finite size of the systems studied. Moreover, the SRO-LRO transition is expected to occur at fairly high Mn concentrations that are inaccessible by usual bulk-growth techniques.¹ The lack of experimental data in the required alloy composition range has in turn seriously impeded the development of any analytical theory concerning a possible SRO-LRO transition in these systems.

We have overcome the limitations on alloy composition by using the nonequilibrium growth technique of molecular-beam epitaxy (MBE) and report here the observation by neutron diffraction of a true second-order antiferromagnetic phase transition in single-crystal zinc-blende epitaxial layers of $\text{Cd}_{1-x}\text{Mn}_x\text{Se}$ ($x=0.70, 0.75$) grown on GaAs(100) by MBE. The main purpose of this Brief Report is to demonstrate that magnetism in these epilayers is dramatically different from what might be expected by simply extrapolating to higher Mn concentrations the behavior observed so far in bulk samples. We should point out that the various II-VI DMS alloys, although chemically different, are very similar as far as their basic properties are concerned.¹ Hence, the implications of the present study are not restricted to $\text{Cd}_{1-x}\text{Mn}_x\text{Se}$.

The growth of $\text{Cd}_{1-x}\text{Mn}_x\text{Se}$ epilayers on GaAs(100) has been fully described elsewhere.¹¹ While bulk growth restricts $\text{Cd}_{1-x}\text{Mn}_x\text{Se}$ single-crystal samples to the hexagonal wurtzite phase with $0 \leq x \leq 0.5$, MBE permits the isolation of single-phase zinc-blende crystals with substantially higher Mn concentrations. This has been demonstrated by detailed characterization of such epilayers by x-ray diffraction and transmission electron microscopy

(TEM),¹¹ as well as by Raman spectroscopy.¹² The samples examined in the present neutron-diffraction study had compositions $x=0.40, 0.54, 0.70,$ and $0.75,$ as deduced from lattice parameter measurements. The epilayers were restricted to thicknesses between 1.5 and $2 \mu\text{m}.$ ¹³ Since the critical thickness for strained-layer pseudomorphic growth of $\text{Cd}_{1-x}\text{Mn}_x\text{Se}$ epilayers is well under $1 \mu\text{m},$ the lattice mismatch between the substrate and the epilayers (ranging from 4 to 5% for the samples studied) is relieved by the formation of dislocations. Measurements of the in-plane and out-of-plane lattice parameters using both x-ray diffraction and neutron diffraction indicate no detectable tetragonal distortion. Apart from dislocations generated by the mismatch, TEM studies indicate the formation of stacking faults, typically spaced at intervals of $300\text{--}500 \text{ \AA}.$

Neutron-diffraction measurements were carried out at the 20 MW research reactor of the National Institute of Standards and Technology, using a triple axis spectrometer with a (002) pyrolytic graphite (PG) monochromator and analyzer, and a PG filter in the incident beam. An analyzer fixed for elastic scattering was used to reduce the large inelastic incoherent background from the GaAs substrate on which $\text{Cd}_{1-x}\text{Mn}_x\text{Se}$ was grown. The energy used was $14.8 \text{ meV},$ with $40'$ collimation throughout the spectrometer for most of the data. The samples were placed in a variable-temperature cryostat, and were oriented with the scattering plane coincident with the (001) crystal plane, and hence perpendicular to the (100) surface of the epilayer. This enabled the observation of the $(hk0)$ reflections. By rotating the crystal by 90 about the [100] direction so as to make the scattering plane coincide with the (010) crystal plane, we could also observe the $(h0l)$ reflections.

Neutron-diffraction measurements in $\text{Cd}_{1-x}\text{Mn}_x\text{Se}$

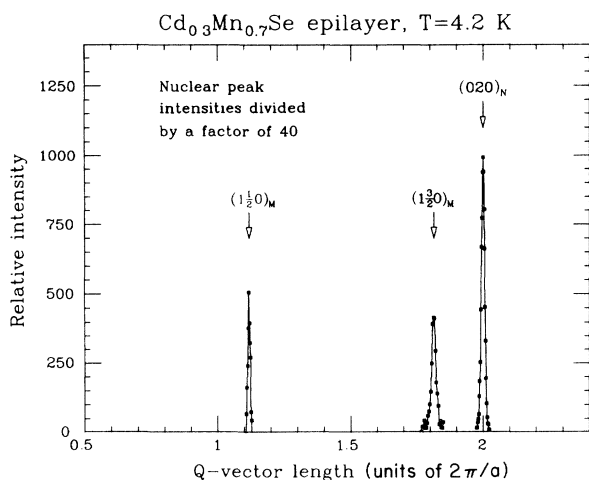


FIG. 1. Nuclear peak $(0,2,0)$ and magnetic peak $(1, \frac{1}{2}, 0)$ and $(1, \frac{3}{2}, 0)$ corresponding to AFM-III order for the $\text{Cd}_{0.3}\text{Mn}_{0.7}\text{Se}$ epilayer. The scans were carried out for the longitudinal direction. The peaks are plotted as a function of the magnitude of the \mathbf{Q} vector. The counting time per point for the data displayed was approximately 28 min ($10'-10'-10'-20'$ configuration). The magnetic peaks are plotted with the background subtracted.

epilayers with $x=0.70$ and 0.75 reveal that, below a well-defined critical temperature $T_N,$ additional diffraction maxima are observed corresponding to magnetic AFM-III superstructure points, as shown in Fig. 1, where one nuclear and two magnetic reflections are shown as a function of the magnitude of the \mathbf{Q} vector. The AFM-III spin lattice has a tetragonal magnetic unit cell, corresponding to a doubling of the crystallographic fcc unit cell along one of the cubic axes. The allowed (hkl) reflections for this structure (using the cubic coordinate system) have an odd half-integer index $n/2$ referring to the doubling direction (with $n=1, 3, 5, \dots$), and of the remaining indices one is even and one is odd [e.g. $(\frac{1}{2}, 2, 1)$]. We thus observe three families of reflections at $(n/2, k, l)$ $(h, n/2, l),$ and $(h, k, n/2)$ points, arising from domains with the tetragonal axes oriented, respectively, along the [100], [010], and [001] directions.

The first striking aspect of the AFM-III order observed in the present data is the LRO shown by domains with the tetragonal axis within the epilayer plane. In experiments on bulk crystals, the magnetic superstructure peaks are much broader than the nuclear peaks, and Lorentzian in shape, indicating short-range AFM-III correlations. Estimated values of the correlation lengths (obtained from the widths of the Lorentzian peaks) for various bulk-grown DMS single-crystal samples are summarized in Fig. 2. In stark contrast, the AFM-III peaks shown in Fig. 1 are comparable in width to the nuclear peaks and are Gaussian, corresponding to LRO.

In order to establish the scale of the magnetic correlations for the long-range (in-plane) domains, we carried out a series of measurements with the beam collimations

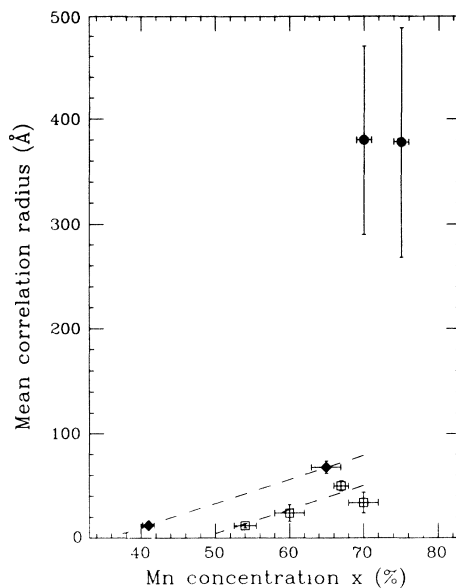


FIG. 2. Summary of maximum estimated correlation lengths observed in all DMS alloys studied to date. Diamonds and open squares represent bulk crystal data for CdMnTe and $\text{ZnMnTe},$ respectively; solid circles at the upper right-hand side represent the present results on CdMnSe epilayers. Note the dramatic difference between the correlation lengths observed in the present study and in earlier studies on bulk crystals.

tightened to $10'-10'-10'-20'$, which gave a Q resolution $\delta Q_t = 0.0025 - 0.004 \text{ \AA}^{-1}$ for the transverse scanning direction and $\delta Q_l = 0.0085 - 0.011 \text{ \AA}^{-1}$ for the longitudinal scanning direction. In this case both the nuclear and the magnetic peaks are broader than the spectrometer resolution, allowing a quantitative determination of the effective nuclear and magnetic linewidth. The intrinsic linewidths of the (200), (020), and (220) nuclear reflections obtained for a $\text{Cd}_{1-x}\text{Mn}_x\text{Se}$ epilayer by deconvoluting the resolution function were, respectively, $\delta Q_t = 0.025, 0.011, \text{ and } 0.022 \text{ \AA}^{-1}$, and $\delta Q_l = 0.021, 0.017, \text{ and } 0.023 \text{ \AA}^{-1}$. The widths of the $(1, \frac{1}{2}, 0)$ and $(1, \frac{3}{2}, 0)$ magnetic reflections obtained for the same sample were, respectively, $\delta Q_t = 0.012 \text{ and } 0.017 \text{ \AA}^{-1}$, and $\delta Q_l = 0.020 \text{ and } 0.021 \text{ \AA}^{-1}$. From these measurements, we estimate the AFM-III correlation length of the "in-plane" domains to be $380 \pm 85 \text{ \AA}$ for $x = 0.70$. A similar value (380 ± 110) \AA is obtained for $x = 0.75$ (the error here is slightly larger due to lower Q resolution in the measurements). In other words, the AFM-III correlations are long-range in character, and appear to be limited only by the crystallographic coherence of the $\text{Cd}_{1-x}\text{Mn}_x\text{Se}$ lattice itself.¹⁴ Figure 2 clearly shows that the measured correlation length cannot be explained by simply extrapolating the trend observed in bulk crystals.

Epilayers with $x = 0.40$ and 0.54 do not show evidence of magnetic peaks. This is attributed to the fact that at these concentrations only SRO is possible, which results in insufficient neutron intensity. While this is not a problem in bulk samples of comparable Mn concentration, the thin epilayers suffer from a large incoherent background signal from the GaAs substrate that probably overwhelms any detectable scattering from the very short-range correlations expected in these samples.

The second important aspect of the present data is the temperature dependence of the magnetic peaks. In bulk crystals, very broad magnetic diffraction peaks signaling short-range AFM-III correlations start developing at relatively high temperatures (even as high as 300 K).⁸ These peaks gradually narrow with decreasing temperature, eventually saturating at widths corresponding to correla-

tion lengths of, at most, 70 \AA . In contrast, the AFM-III peaks in the present case appear at a well-defined transition temperature, below which the width of these peaks is temperature independent. On the other hand, the intensity of the peaks increases with decreasing temperature, following a square Brillouin function for $S = \frac{5}{2}$, as shown in Fig. 3. This strongly suggests a second-order antiferromagnetic phase transition, consistent with the observed LRO and the mean-field approximation. The onset of LRO occurs at a Néel temperature of $T_N = 56 \text{ K}$ for $x = 0.70$. The value of T_N for $x = 0.75$ is indistinguishable from that for $x = 0.70$ within experimental error.

A final comment concerns the observation of anisotropy in the AFM-III correlations. As might be expected for cubic structures, the neutron spectra obtained for bulk DMS crystals indicate an equal population and equal correlation range for the three orthogonal AFM-III domain orientations. In contrast, the experiments on $\text{Cd}_{1-x}\text{Mn}_x\text{Se}$ epilayers reveal striking differences between the $(n/2, k, 0)$ reflections (i.e., those arising from domains with the tetragonal axis normal to the epilayer plane) and $(h, n/2, 0)$ and $(h, 0, n/2)$ reflections arising from domains with the in-plane axis orientation. The domains with the tetragonal axis perpendicular to the epilayer plane clearly show SRO ($< 100 \text{ \AA}$), while domains with tetragonal axes in the epilayer plane, as explained earlier, develop LRO. The origin of this anisotropy is not presently understood.

In summary, elastic neutron scattering measurements provide clear evidence for a second-order antiferromagnetic phase transition in $\text{Cd}_{1-x}\text{Mn}_x\text{Se}$ epilayers with $x \geq 0.70$. The AFM-III in these samples is distributed amongst three orthogonal domain orientations, with LRO being manifested only by domains with the tetragonal axis oriented within the epilayer plane. As suggested by Fig. 2, the LRO cannot be attributed solely to the high Mn concentration in these epilayers. It is likely that the onset of LRO is the combined effect of both the high Mn concentration and residual strain that is not detected by in-plane and out-of-plane lattice parameter measurements. The latter factor can lead to a finite tetragonal distortion, resulting in differing exchange interactions within the epilayer plane and normal to it. Such an anisotropy in the exchange, though small, might be sufficient to break the degeneracy of states inherent in AFM-III domains in an undistorted fcc lattice. The presence of such an anisotropy is strongly suggested by the preference for LRO domains with an in-plane tetragonal axis. However, the lattice parameter of $\text{Cd}_{1-x}\text{Mn}_x\text{Se}$ is *larger* than that of the GaAs substrate, and any strain-related exchange anisotropy should actually favor the stabilization of domains with tetragonal axis *normal* to the layer plane. Further experimental measurements on $\text{Cd}_{1-x}\text{Mn}_x\text{Se}$ epilayers with $0.60 \leq x \leq 0.70$ are planned in order to resolve these questions. It is also hoped that the results here will be complemented by other magnetic probes, such as magnetization and spin-flip Raman measurements, as well as theoretical calculations, in order to clarify the magnetic behavior in this new system.

This work was supported by National Science Foundation Grant No. DMR-8821635.

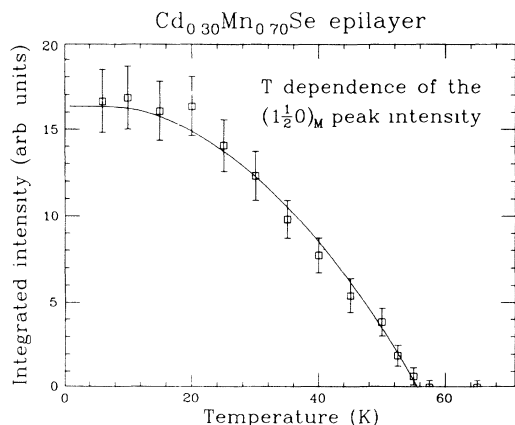


FIG. 3. Experimental peak intensity of the $(1, \frac{1}{2}, 0)$ reflection in a $\text{Cd}_{0.3}\text{Mn}_{0.7}\text{Se}$ epilayer as a function of temperature. The solid curve is a fit of the data to the squared Brillouin function for $S = \frac{5}{2}$ and gives a Néel temperature of 56 K.

- *Also at the National Institute of Standards and Technology, Gaithersburg, Maryland 20899.
- ¹J. K. Furdyna, *J. Appl. Phys.* **64**, R29 (1988).
- ²C. L. Henley, *Phys. Rev. Lett.* **62**, 2056 (1989).
- ³B. E. Larson, K. C. Hass, H. Ehrenreich, and A. E. Carlsson, *Solid State Commun.* **56**, 347 (1985).
- ⁴See J. K. Furdyna and N. Samarth, *J. Appl. Phys.* (to be published), and references therein.
- ⁵M. Ayadi, J. Ferre, A. Mauger, and R. Triboulet, *Phys. Rev. Lett.* **57**, 1165 (1986).
- ⁶S. Geschwind, A. T. Ogielski, G. E. Devlin, J. Hegarty, and P. Bridenbaugh, *J. Appl. Phys.* **63**, 3738 (1988).
- ⁷S. Geschwind, D. A. Huse, and G. E. Devlin, *Phys. Rev. B* **41**, 4854 (1990); see also *ibid.* **41**, 2650 (1990).
- ⁸T. M. Giebultowicz and T. M. Holden, in *Diluted Magnetic Semiconductors*, edited by J. K. Furdyna and J. Kossut (Academic, Boston, 1988).
- ⁹C. L. Henley, *J. Appl. Phys.* **61**, 3962 (1987).
- ¹⁰T. Giebultowicz, *J. Magn. Magn. Mater.* **54-57**, 1287 (1986).
- ¹¹N. Samarth, H. Luo, J. K. Furdyna, Y. R. Lee, R. G. Alonso, E. K. Suh, A. K. Ramdas, S. B. Qadri, and N. Otsuka, *Surf. Sci.* (to be published). See also N. Samarth, H. Luo, J. K. Furdyna, S. B. Qadri, Y. R. Lee, A. K. Ramdas, and N. Otsuka, *Appl. Phys. Lett.* **54**, 2680 (1989).
- ¹²R. Alonso, E. K. Suh, A. K. Ramdas, N. Samarth, H. Luo, and J. K. Furdyna, *Phys. Rev. B* **40**, 3720 (1989).
- ¹³Layers thicker than 2 μm show rapid deterioration of crystal quality, while we estimate that layers much thinner than 1.5 μm would not provide sufficient neutron scattering intensity.
- ¹⁴We note that, as a result of crystalline defects (stacking faults and dislocations) mentioned earlier, the nuclear peaks observed in the epilayer are somewhat broader than those observed in high-quality defect-free crystals, such as the GaAs substrate.